Influence of interelectrode distances in electrocoagulation: is there any possibility and advantages to operate at micro-distances with low-conductivity effluents?

Emmanuel Mousset, Faidzul Hakim Adnan, Aurélien Ruffet, Paul Moretti, Bruno Cédat

Influence of interelectrode distances in electrocoagulation: is there any possibility and advantages to operate at micro-distances with low-conductivity effluents?

Emmanuel Mousset[1,2,*], Faidzul Hakim Adnan[1], Aurélien Ruffet[1,3], Paul Moretti[3], Bruno Cédat[3]

[1] *Université de Lorraine, CNRS, LRGP, F-54000 Nancy, France*

[2] *Nantes Université, ONIRIS, CNRS, GEPEA, UMR 6144, F-85000 La Roche-sur-Yon, France*

[3] *Treewater, 61 Rue de la République, 62009 Lyon, France*

***CHEMOSPHERE* JOURNAL**

*Contact of corresponding author:emmanuel.mousset@cnrs.fr

Graphical abstract

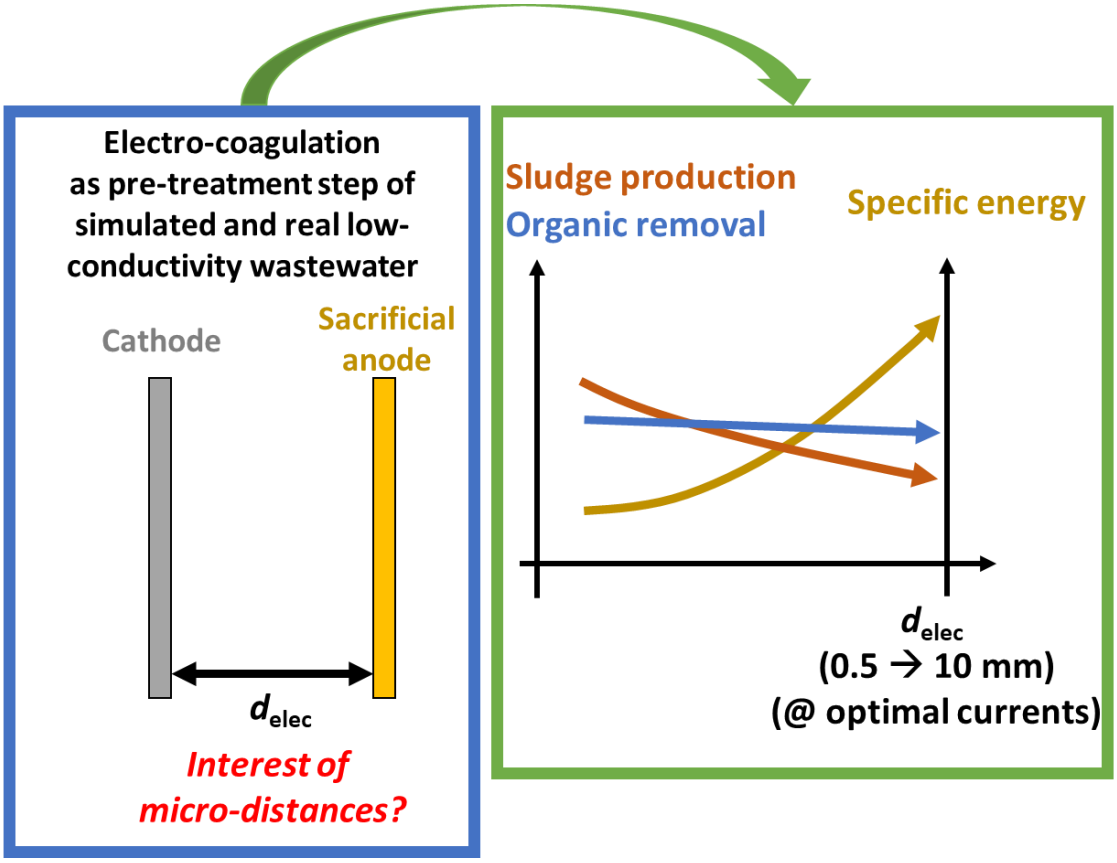

Highlights

- Total organic carbon removal was noticed even at micro-distances (100 – 500 μm)
- Higher energy efficiency with low-conductivity effluent with micro-distances
- Higher sludge generation with micro-distances due to higher current requirement
- Aluminium anode could not be implemented with microfluidic filter-press configuration

List of symbols, abbreviations and nomenclatures

Nomenclature/ symbols/ acronyms/ abbreviations	Definition
	Nomenclature
$[\text{paracetamol}]_0$	Initial concentration of paracetamol
	Symbols
d_{elec}	Interelectrode distance
E_{sp}	Specific energy
I_{app}	Applied current intensity
j_{app}	Applied current density
	Acronyms/Abbreviations
EC	Electrocoagulation
IC	Ion chromatography
ICP-OES	Inductively coupled plasma optical emission spectroscopy
HPLC	High-performance liquid chromatography
PTFE	Polytetrafluoroethylene
TIC	Total inorganic carbon
TIN	Total inorganic nitrogen
TOC	Total organic carbon
UV	Ultraviolet

Abstract

It is proposed for the first time to investigate the possibility to implement micro-inter-electrode distances in electrocoagulation (EC) in order to improve both the treatment and energy efficiencies compared to conventional EC cells with centimetric distances. The study has been performed in a microfluidic monopolar flow-by filter-press cell for the treatment of simulated and real low-conductivity (0.5 - 1 mS cm^{-1}) laundry wastewaters. The influences of interelectrode distance (d_{elec}) (100 - 10,000 µm), applied current density (j_{app}) (10 - 200 mA cm^{-2}), and types of anode materials (iron, aluminium and stainless steel) have been studied. The removal of representative organic pollutant (i.e., paracetamol at 15 mg L^{-1}) as well as of total organic carbon (TOC) content (312 mg-C L^{-1}) from actual wastewater was noticed, including at micro-distances. Optimal treatment capacities were obtained with d_{elec} of 0.5 mm (57% TOC removed), 3 mm (58% TOC removed) and 10 mm (41% TOC removed) and with j_{app} of 70 mA cm^{-2}, 40 mA cm^{-2} and 20 mA cm^{-2} respectively, using stainless steel anode. It led to reduced energy requirement at micro-distances (16 kWh g-TOC^{-1} at 500 µm) compared to millimetric gap (19 kWh g-TOC^{-1} at 3 mm, 40 kWh g-TOC^{-1} at 10 mm). Contrastingly, more sludge was generated with micrometric distance (172 g-sludge g-TOC^{-1} at 500 µm) compared to larger gaps (95 g-sludge g-TOC^{-1} at 3 mm, 87 g-sludge g-TOC^{-1} at 10 mm) due to higher optimal j_{app} at low distances. The efficiency was maximal with an aluminium electrode, but this anode remained inapplicable with micro-distances using the current reactor design, given the high sludge production between the cathode and anode.

Keywords:

Anode materials; electrodissolution; electro-oxidation; low-conductivity effluents; microfluidic reactor; real industrial wastewater

1. Introduction

Various sectors of the economy lead to the production of increasingly complex wastewater that are increasingly loaded with bio-recalcitrant compounds (Richardson and Ternes, 2014; Moussa et al., 2017; Mousazadeh et al., 2021). However, the conventional treatments, such as bioprocesses, used in wastewater treatment plants are not completely effective in treating these compounds (Rizzo et al., 2020). It is therefore necessary to study and propose an alternative or complementary treatment to conventional water treatment systems. These alternatives must be environmentally friendly while being more effective at a lower cost.

Among these alternatives, there are electrochemical treatments. They are very versatile, simple to implement and can be carried out without the addition of chemical reagents (Radjenovic and Sedlak, 2015; Mousset and Hatton, 2022; Deng et al., 2023; Mousset et al., 2023; Puthiya Veetil Nidheesh et al., 2023; P. V. Nidheesh et al., 2023). The interest of using inter-electrode distance (d_{elec}) in the micrometric range (< 1 mm) has been demonstrated in the field of water treatment by electro-oxidation (Scialdone et al., 2010; Pérez et al., 2018a; Adnan et al., 2022a, 2021a). Low d_{elec} improve the mass transport and electronic exchange between electrodes which can increase the efficiency of the treatment and reduce the energy requirement (Scialdone et al., 2011, 2014; Mousset, 2020; Adnan et al., 2021b, 2022b, 2022c, 2023). It also permits to operate electrolysis with low-conductivity wastewater without the need for electrolyte addition (Ma et al., 2018; Diris et al., 2024). Moreover, there is the need to combine conversion technologies with separation techniques in order to benefit from synergies in a complete treatment train, to ensure an efficient removal of pollutants and unwanted by-products (Ren et al., 2018; Mousset and Hatton, 2022; Mousset et al., 2023).

Electrocoagulation (EC) is one of the electrochemical technologies that is increasingly considered as a viable alternative to certain conventional pre-treatment step (e.g. chemical coagulation-flocculation) thanks to its efficiency in eliminating both suspended solids in water and colloidal suspensions, as well as a fraction of dissolved compounds (Canizares et al., 2008; Cañizares et al., 2009; Garcia-Segura et al., 2017; Hakizimana et al., 2017; Flores et al., 2018; Jing et al., 2021; AlJaberi et al., 2022; Aiyd Jasim

and AlJaberi, 2023; AlJaberi, 2023; Vargas et al., 2023). Several cell designs have been previously explored, including porous three-dimensional electrode implemented (or not) as bed electrode reactor (Wang et al., 2020; Song et al., 2022; Li et al., 2023), as well as flow-by cells with parallel plate electrodes. In the latter one, the design implies a better control of the d_{elec} as well as of the potential of electrode and an enhanced homogeneity of potential distribution compared to bed reactor and 3D electrodes, in monopolar mode (Lissaneddine et al., 2022).

The d_{elec} has previously shown having an influence on the efficiency of EC, particularly in such flow-by cells. The literature suggests better removal rates for d_{elec} between 5 mm (Sánchez Calvo et al., 2003; Kabdaşlı et al., 2012; Attour et al., 2014) and 10 mm (Mousazadeh et al., 2021), but without having compared the results with a configuration involving micro-distances. It could be expected that at very low d_{elec}, metal hydroxides could interact preferentially with each other rather than with pollutants (Khandegar and Saroha, 2013). Under these conditions, the pressure drop would be very high, which would limit the applicable flow rate range and the risk of clogging could increase drastically. Thus, the treatment capacity could also decrease. Contrastingly, the mass transfer between electrodes decreases when d_{elec} increases and the energy requirement could be lower, which would make the process more economically advantageous. Therefore, a compromise is necessary and implies the existence of an optimal distance that need to be determined considering a wider range of d_{elec}. Furthermore, the implementation of micro-distances with low-conductivity solution such as laundry effluents (Feng et al., 2021; Khalid et al., 2022; Arbid et al., 2024; Khajvand et al., 2024) would be beneficial, particularly in terms of energy requirement.

Hence the motivation of this work was to compare for the first time the EC efficiency between optimized macrometric and micrometric distances configurations, by varying the applied current density (j_{app}), with low-conductivity solution ranging from 0.5 to 1 mS cm^{-1}. Investigating a wide range of d_{elec} within the same study has ensured a more suitable comparison between micrometric distances and centimetric distances that are commonly implemented in literature (Janpoor et al., 2011; Feng et al., 2021;), since all the other parameters of the system (reactor design, electrode surface/treated volume ratio, effluent characteristics) were the same. Through these studies, different electrode materials such as stainless

steel, iron and aluminum were tested to verify their treatment efficiency by gradually increasing the degree of complexity of the medium, starting with synthetic effluents containing representative pollutants, then studying a real industrial effluent such as laundry wastewater that has never been tested in such micro-distances mode, on the contrary to centimetric distances (Janpoor et al., 2011; Feng et al., 2021). The elimination rates of the organic compound and the overall organic fraction were evaluated in different configurations while monitoring energy consumption and the formation of undesirable inorganic by-products.

2. Material and Methods

2.1. Effluents characteristics

As a first approach, a synthetic effluent has been studied and was containing paracetamol (15 mg L^{-1}) (99%, Sigma-Aldrich) as representative organic pollutant from wastewater. The selected electrolyte was sodium sulfate (Na_2SO_4) (568 mg L^{-1}) (> 97%; Carlo Erba, Val de Reuil, France) for experiments in the presence of only the pharmaceutical compound in ultrapure water at 18.2 MΩ.cm (PureLab ELGA Classic, Veolia Water, Antony, France). The use of Na_2SO_4 has been used as non-electroactive electrolyte in order to limit the interferences on the mechanisms of EC.

A real industrial effluent was collected from a laundry located in France, whose physicochemical characteristics, which includes total organic carbon (TOC), total inorganic carbon (TIC) and total inorganic nitrogen (TIN), is described in **Table S1**. This effluent has been selected as a second approach to assess the matrix effect with an actual wastewater as case study.

2.2. Electrolysis setup

A filter press type electrochemical reactor was used and its characteristics have been already detailed previously (Adnan et al., 2021a, 2021b). The planar anode and cathode were arranged in parallel and vertically. A polytetrafluoroethylene (PTFE) (Bohlender, Grünsfeld, Germany) spacer was used to separate the anode and the cathode; varying its thickness determined the d_{elec} of the EC reactor.

The electric current was applied using a power supply (HAMEG, Rohde & Schwarz). A range of j_{app} from 10 to 200 mA cm^{-2} (corresponding to applied current intensity (I_{app}) varying from 0.5 to 10 A) was varied throughout this work. The study of the influence of d_{elec} on the efficiency of the EC process was carried out using d_{elec} of 0.1, 0.5, 3, 5 and 10 mm by varying j_{app} for getting optimal current value at each d_{elec}, since it has been previously shown that d_{elec} and j_{app} are strongly correlated (Diris et al., 2024). A 316L stainless steel (Gantois, France) material was mainly used as both cathode and anode to study the effect of d_{elec} and j_{app}, with the synthetic effluent containing paracetamol.

The EC efficiency using stainless steel electrodes was compared with iron (99.85%; Berthelot SAS, France) and aluminum (99.5%; Barthelot SAS, France) electrodes to study the effect of electrode materials. This was done with laundry effluent, while iron, stainless steel, and aluminum materials were used as paired electrodes (i.e., the same material was implemented as both cathode and anode), at the optimal working conditions determined in the studies on the d_{elec} and j_{app} combined effects. Therefore, the influence of electrode materials has been assessed at different combinations of d_{elec} and j_{app}. All electrode materials (cathodes and anodes) had the same geometric surface (50 cm^2) in contact with the liquid, which was the surface considered for j_{app} calculation.

The stainless steel electrode was immersed in 0.25 M sulfuric acid solution overnight after each run, in order to dissolve any precipitates and remove the passive layer potentially formed on the electrode surface (Adnan et al., 2021a). After each use, the iron and aluminum electrodes were sanded with abrasive paper to remove the passivation layer that had formed on their surfaces. They were then rinsed with acetone followed by a thorough cleaning step with ultrapure water (Ezechi et al., 2020).

A platinum (90%)/iridium (10%) (Pt) anode (Ögussa, Vienna, Austria), with 50 cm^2 of geometric surface exposed to water, has been used in control experiments, paired with stainless steel cathode, in order to decouple the general mechanism, by carrying out the influence of direct oxidation on the global removal efficiency.

The volume of effluent to be treated in each experiment was 500 mL. The circulation of the effluent was ensured by a peristaltic pump (Masterflex, Cole Parmer), whose recirculation flow rate was varied for each d_{elec} in order to ensure the conservation of the residence time (Adnan et al., 2021a, 2021b). Thus, a circulation flow rate of 0.02, 0.1, 0.6 and 1 L min^{-1} was used for distances of 0.1, 0.5, 3 and 5 mm respectively. For these d_{elec}, the treatment time was 2 h. The recirculation flow rate for a distance of 10 mm was the same as that for a distance of 5 mm (1 L min^{-1}) and the residence time was doubled (4 h) in order to keep the same number of passes as for the lower d_{elec} (**Table S2**).

2.3. Analytical methods

Inductively coupled plasma optical emission spectroscopy (ICP-OES) (Thermo iCAP 6000; Thermo Fisher, Noisy-le-Grand, France) was used to determine the concentrations of calcium (Ca^{2+}) and magnesium (Mg^{2+}) ions. These were assumed to be equivalent to the concentrations of Ca and Mg elements measured by ICP-OES (Adnan et al., 2021a). Mg and Ca were quantitively detected by OES with the respective wavelengths: 79.55, 280.27 and 285.21 nm for Mg and 317.93, 318.12 and 422.67 nm for Ca. The calibration was performed externally by varying concentrations of Mg from 0.5 to 5 mg L^{-1} and Ca from 5 to 50 mg L^{-1}, using ICP-OES standard solution at 1000 mg L^{-1}. ICP-OES samples were obtained by collecting 0.5 mL of effluent, which was then filtered at 0.45 µm (Phenex™; Phenomenex, Le Pecq, France) and acidified with a 0.5 M sulfuric acid solution, using a dilution factor of 10.

High-performance liquid chromatography (HPLC) coupled to a diode array detector was used to monitor the evolution of the concentration of the paracetamol molecule. It was performed in isocratic mode with a C18 column (Phenex, France). All samples were filtered at 0.45 µm (Phenex™). A Kinetex® reversed phase C18 column was used (2.6 µm average particle size, 4.6 mm internal diameter, 100 mm length; Phenomenex, Le Pecq, France). The mobile phase consisted of a mixture containing 95% of ultrapure water (containing 1% formic acid) and 5% acetonitrile (containing 1% formic acid). The flow rate of the eluent phase was 0.3 mL min^{-1} and the column temperature was set at 25 °C. An external calibration curve was initially performed by varying concentrations of paracetamol from 0.5 to 20 mg L^{-1} in ultrapure water.

A Ultraviolet (UV)-visible spectrophotometer UV-2600 (Shimadzu, Marne-La-Vallée, France) was used to get the spectra with wavelength varying from 200 to 600 nm at incremental step of 1 nm, using paracetamol solutions in order to verify the presence or not of by-products with molecular structure that could absorb light as well. Ultrapure water was used for the reference light, which permit to limit interference from the internal system for each spectra. In addition, blanks were performed for each

experiment using electrolyte solutions in the absence of paracetamol. The absorbance values of the blanks were subtracted to the absorbance values obtained in the presence of paracetamol

The device used to measure TOC was the Shimadzu TOC-VCSH analyzer equipped with the total nitrogen measuring (TNM-1) device to measure total nitrogen in parallel. The samples were filtered using a 0.45 µm syringe filter (Phenex^{TM}). The TOC values were used to estimate the specific energy (E_{sp}) requirement expressed in kWh g-TOC^{-1} (Brillas et al., 2009).

Ion chromatography (IC) (Dionex ICS-6000) (ThermoFisher, Noisy-Le-Grand, France) was used to separate, identify and quantify ions present in a sample. The AS19 IC Dionex^{TM} IonPac^{TM} chromatographic column (ThermoFisher, Noisy-Le-Grand, France) was used for this purpose. The concentrations of chloride (Cl^-), sulfate (SO_4^{2-}), nitrate (NO_3^-), phosphate (PO_4^{3-}), chlorite (ClO_2^-), chlorate (ClO_3^-) and perchlorate (ClO_4^-) ions were monitored by IC. The samples collected were previously filtered at 0.45 µm (Phenex^{TM}). An external calibration curve was performed with standard solutions containing different concentrations of Cl^- (1-300 mg L^{-1}), SO_4^{2-} (1-480 mg L^{-1}), NO_3^- (0.5-30 mg L^{-1}), PO_4^{3-} (0.5-40 mg L^{-1}), ClO_2^- (0.5-30 mg L^{-1}), ClO_3^- (0.5-40 mg L^{-1}) and ClO_4^- (0.5-40 mg L^{-1}) ions.

The sludge produce during EC was collected by centrifugation (5000 rpm for 20 min) after each electrolysis (Rodier et al., 2009). The sludge was then placed in an oven at 105 °C for 24 h before quantifying the dry weight.

3. Results and Discussion

3.1. Effect of interelectrode distance

The effect of a wide range of d_{elec} on the EC efficiency, starting from micro-distances (100 and 500 µm) to millimetric (3 and 5 mm) and centimetric (1 cm) distances has been investigated for the first time. **Figure 1** shows the decay of paracetamol as a function of number of passes and at different d_{elec}.

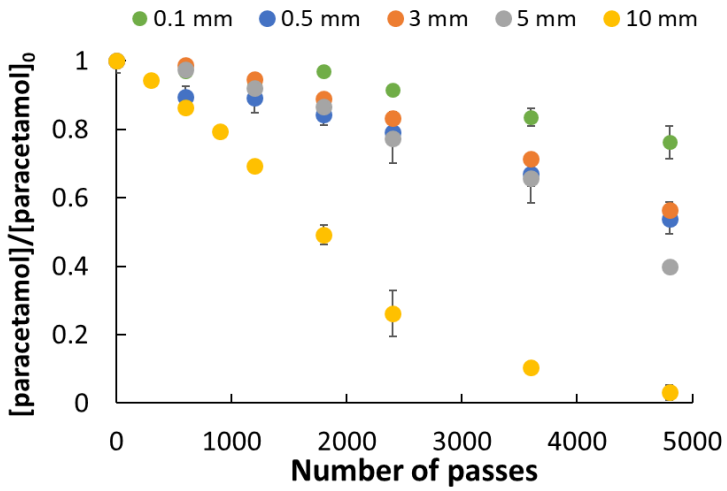

Fig. 1. Decay of paracetamol concentration in synthetic effluent as a function of number of passes and at different d_{elec}. Operating conditions: cathode = stainless steel; anode = stainless steel; $[paracetamol]_0$ = 15 mg L^{-1}, $[Na_2SO_4]$ = 568 mg L^{-1}, j_{app} = 20 mA cm^{-2}.

The paracetamol concentration in the effluent decreased for each d_{elec} value. The greater the distance, the lower the paracetamol concentration in solution at the end of treatment. For a d_{elec} of 5 mm, more than 60% of paracetamol was eliminated after 4800 number of passes. For d_{elec} of 0.5 mm to 3 mm, more than 40% is removed, while 24% of decay was noticed at a d_{elec} of 0.1 mm. With a d_{elec} of 10 mm, the elimination of paracetamol was almost complete after 4 h of electrolysis. Taking only the paracetamol decay into account, the distance that seemed optimal was 10 mm. This was in agreement with the literature in which only centimeter distances and some millimeter distances have been tested (Sánchez Calvo et al., 2003; Attour et al., 2014; Mousazadeh et al., 2021).

However, paracetamol may not only be eliminated by the sludge generated by EC, but also degraded by direct electro-oxidation at the anode. The absorbance peaks obtained during the monitoring of the reaction kinetics by UV-visible spectroscopy allowed to identify this phenomenon. The absorbance peaks are presented in **Fig. S1**. **Figure S1** showed two absorbance peaks. One of the peaks was present initially, whose peak could be initially linked to paracetamol (ʎ = 243 mm). A second peak appeared at the end of the first sampling (15 min), and increased over the course of the reaction. This was the peak attributed to the by-products that are able to absorb light at ʎ around 343 mm. This peak interfered with

the paracetamol peak. Control experiments with a Pt anode were carried out to verify the degradation of paracetamol by direct electro-oxidation at a d_{elec} of 10 mm and j_{app} of 20 mA cm^{-2}. The corresponding paracetamol decay, whose concentrations were determined by HPLC, are displayed in **Fig. S2**. Since EC mechanism cannot occur with a Pt anode in such electrolytic conditions, the decay of paracetamol concentration with Pt anode confirmed that direct electro-oxidation was involved during EC treatment. Considering the small difference of paracetamol removal percentages (between 3 to 10%) between Pt and stainless steel anodes experiments (**Fig. S2**), it could be conclude that electro-oxidation mechanism should be the predominant one occurring during experiments with stainless steel electrodes and paracetamol solutions. It was therefore necessary to check the reduction of the total organic fraction of the solution (TOC), including the potential organic by-products formed.

Figure 2a illustrates the TOC removal percentages obtained during the electrolysis of the synthetic effluent subjected to a j_{app} of 20 mA cm^{-2} and to different d_{elec}. The TOC removal yields increased with d_{elec}, with a more drastic increase between 5 mm and 10 mm. Here again, 10 mm was the d_{elec} giving the best removal (41%), which was in agreement with the trends observed with the paracetamol decay (**Fig. 1**) and with the optimal d_{elec} values presented in the literature (Mousazadeh et al., 2021).

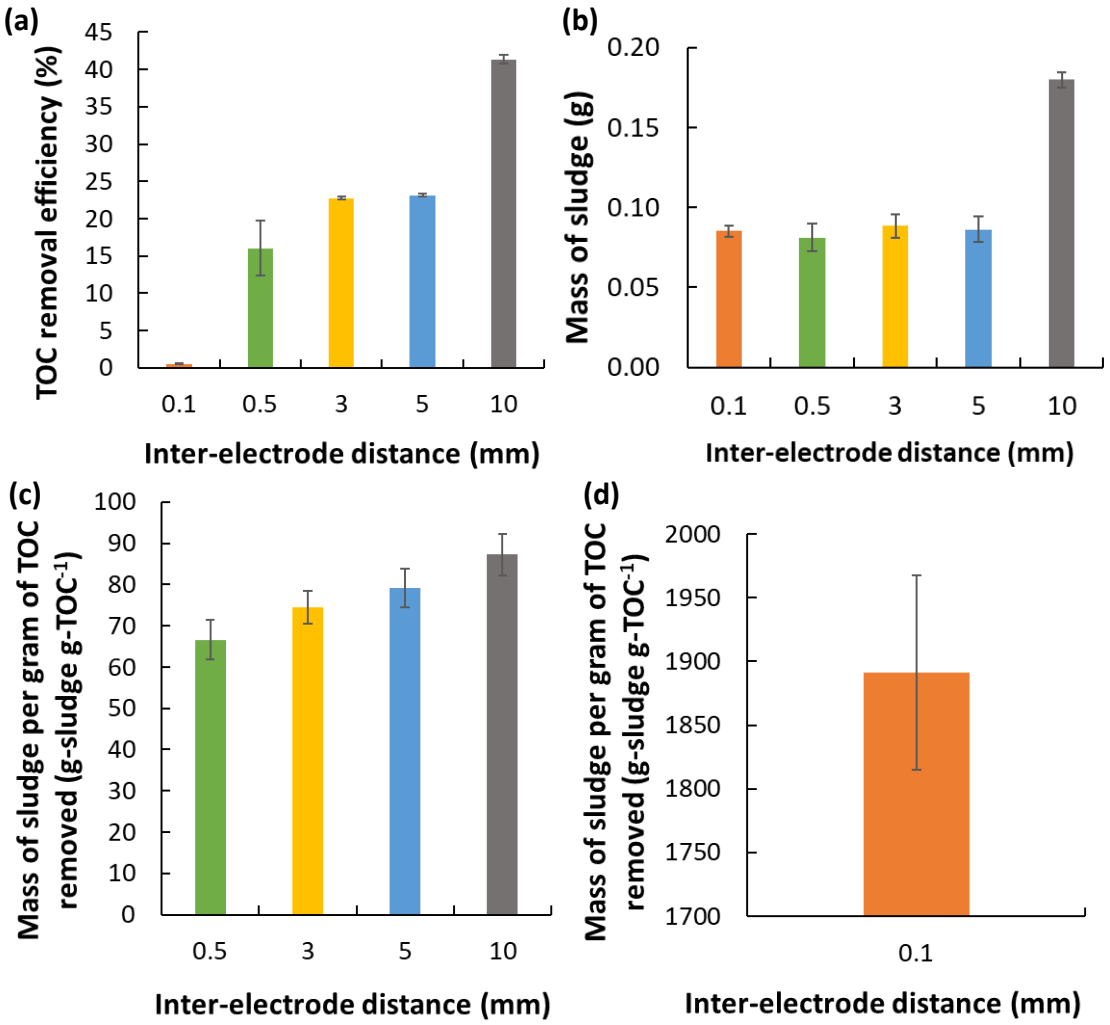

Fig. 2. Effect of d_{elec} on TOC removal yields (a), mass of sludge produced during EC (b), mass of sludge per gram of TOC removed at 0.5, 3, 5 and 10 mm (c), mass of sludge per gram of TOC removed at 0.1 mm (d). Operating conditions: cathode = stainless steel; anode = stainless steel; $[paracetamol]_0$ = 15 mg L^{-1}, $[Na_2SO_4]$ = 568 mg L^{-1}, j_{app} = 20 mA cm^{-2}.

The amount of sludge produced as a function of the d_{elec} is presented in **Fig. 2b**. Sludge production was maximum for the 10 mm d_{elec} (0.20 g) and it did not vary significantly for the other d_{elec} (0.1 - 5 mm) (approximately 0.09 g). At a given j_{app}, the more the d_{elec} increased, the more the anode potential increased and the more the anodic dissolution would be important. This could explain the higher sludge production at 10 mm, as well as the higher paracetamol decay rates by EC and electro-oxidation. **Figure 2c** presents the amount of sludge produced per TOC removed. This parameter evolved in the same way as the two previous ones, except at 0.1 mm. Thus, the highest value was reached with the smallest d_{elec}., whose condition led to very low TOC removal yields (< 1%) and therefore very high sludge production per TOC removed. Once again 10 mm seemed to be the optimal distance, which agreed with the typical distance found in literature in the range of 1 - 3 cm (Janpoor et al., 2011; Mousazadeh et al., 2021).

However, monitoring these parameters was not enough to position oneself. The optimal distance must lead to high energy efficiency. **Figure S3** illustrates the variation in E_{sp} at different d_{elec}. The d_{elec} that allowed the least energy loss was 0.5 mm (6.5 kWh g-TOC^{-1}). Conversely, 0.1 mm was the least profitable d_{elec} (158 kWh g-TOC^{-1}). The results could be explained once again by the low rate of TOC removal at this distance. Between 0.5 mm and 10 mm, the E_{sp} was increasing until around 40 kWh g-TOC^{-1}. Therefore, the d_{elec} of 0.5 mm seemed to be interesting compared to 10 mm in terms of energy requirement.

Figure S4 presents the evolution of pH and conductivity of the synthetic effluent containing paracetamol during treatment. According to **Fig. S4a**, the pH of the synthetic effluent decreases and eventually stabilizes around 6, regardless of the d_{elec} used. This trend is not in full agreement with what could be found in the literature. The initial pH of the studied matrix is rather neutral and it is supposed to remain stable over time. A possible explanation could be the nature of the pollutant. Indeed, this decrease in pH could be an inherent property of the pharmaceutical compound, as previously demonstrated with phenolic molecules (Mousset et al., 2016). Since paracetamol has been partly electro-oxidized at the anode (**Fig. S2**), the formation of carboxylic acids by-products could acidify and buffer the environment as previously observed with the electrolytic treatment of phenolic compounds (Mousset et al., 2016).

Figure S4b shows that the ionic conductivity remains relatively stable and reaches a value close to 0.9 mS cm^{-1}, with all distances, except at 0.1 mm. At this distance, the ionic conductivity decreases to around 0.45 mS cm^{-1} and increases again to reach a value of 0.8 mS cm^{-1} after 2 h of electrolysis. At 500 µm, a slight variation in conductivity is observed during the first hour of electrolysis as well, but to a lesser extent than at 100 µm. Micro-distances therefore seem to slightly influence the ionic conductivity of the effluent during EC.

To summarize, the d_{elec} greatly influences the efficiency of the EC. In this part, two distances seemed interesting, depending on the criteria taken into account. Indeed, the d_{elec} of 10 mm allowed to have the best pollutant elimination rate, while the d_{elec} of 0.5 mm was optimal from an energy point of view. This is in agreement with the literature saying that small distances favor energy efficiency (Scialdone et al., 2013; Sabatino et al., 2016; Pérez et al., 2017, 2018b; Rodríguez et al., 2018; Adnan et al., 2022c). Knowing that the electrode potentials vary with d_{elec} (Scialdone et al., 2013; Sabatino et al., 2016; Pérez et al., 2017, 2018b; Rodríguez et al., 2018; Adnan et al., 2022c), it seems important to vary j_{app} for each d_{elec} in order to optimize the current for each distance for a better optimization approach, as proposed in the following section.

3.2. Effect of current density at each interelectrode distance

The evolution of paracetamol concentration as a function of d_{elec} and j_{app} is shown in **Fig. 3**. The optimal current to be applied for total elimination of paracetamol varied according to the d_{elec} value used. Indeed, for a d_{elec} of 10 mm, a j_{app} of 20 mA cm^{-2} was sufficient to completely eliminate paracetamol, while for d_{elec} between 0.1 mm and 5 mm it was necessary to reach 70 mA cm^{-2}. For d_{elec} between 3 mm and 5 mm, if complete elimination of the pollutant is not sought, then a j_{app} of 40 mA cm^{-2} was sufficient to reach 93% of elimination. It was also highlighted that all d_{elec} were potentially interesting in terms of removal efficiency, as long as the right j_{app} was applied. The more j_{app} increased, the greater the elimination of the pollutant. Similarly, the more j_{app} increased, the shorter the treatment time required for complete elimination of the pollutant. These observations were in accordance with Faraday's law involved in EC mechanisms (Hakizimana et al., 2017).

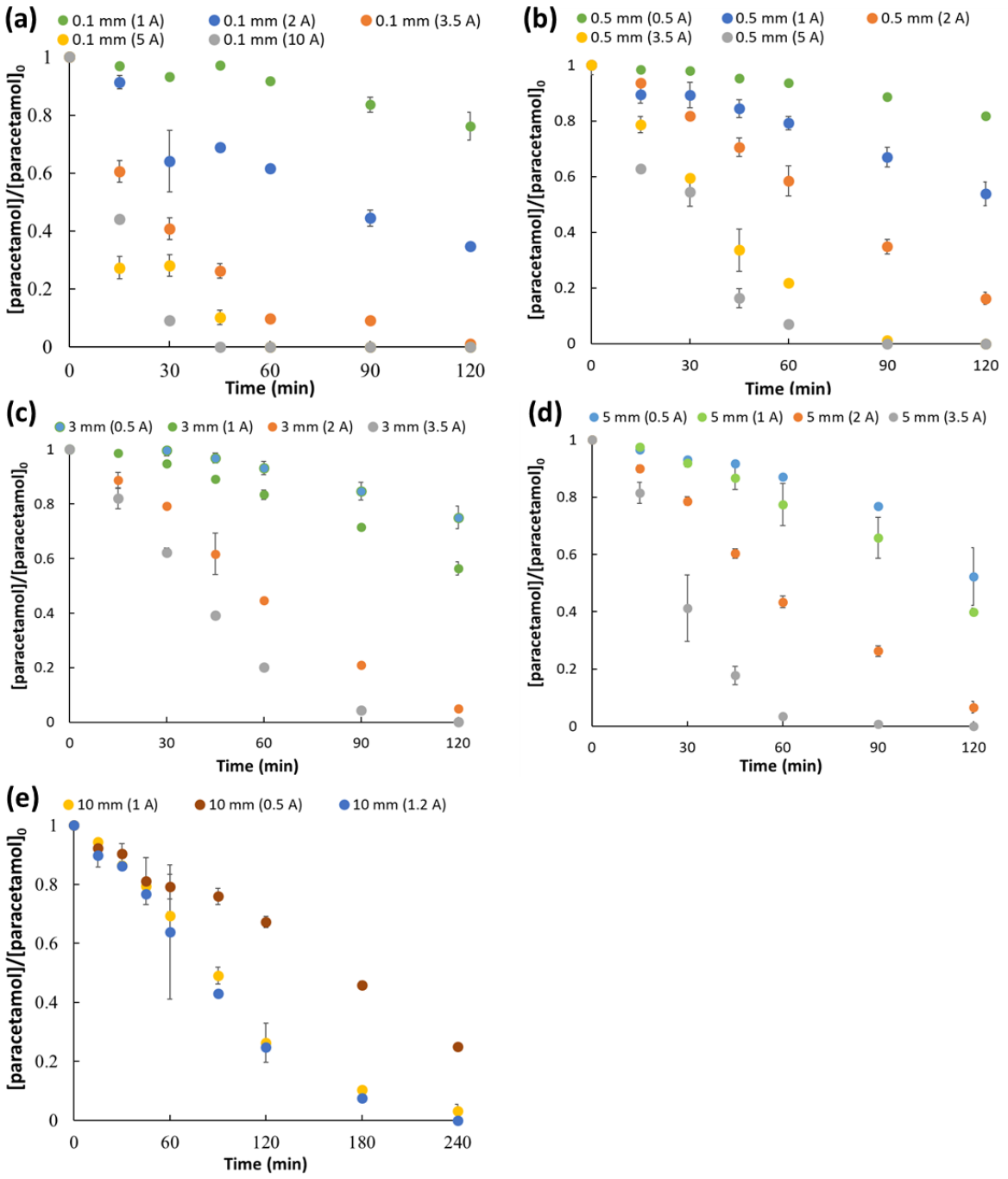

Fig. 3. Decay of paracetamol in synthetic effluent as a function of time at different I_{app} (0.5 A (10 mA cm^{-2}), 1 A (20 mA cm^{-2}), 1.2 A (24 mA cm^{-2}), 2 A (40 mA cm^{-2}), 3.5 A (70 mA cm^{-2}), 5 A (100 mA cm^{-2}), 10 A (200 mA cm^{-2})) and d_{elec}: (a) 0.1 mm, (b) 0.5 mm, (c) 3 mm, (d) 5 mm, (e) 10 mm. Operating conditions: $[paracetamol]_0$ = 15 mg L^{-1}, $[Na_2SO_4]$ = 568 mg L^{-1}.

The variations of the TOC removal rates as a function of d_{elec} and j_{app} are presented in **Fig. 4** and it shows that the TOC reduction increases with increasing d_{elec} and j_{app}. The highest reduction value (60%) is achieved with 200 mA cm^{-2} (10 A) for a distance of 0.1 mm. Furthermore, a j_{app} of 70 mA cm^{-2} (3.5 A) was sufficient to reduce the organic content by half at this distance, whereas for a d_{elec} value between 0.5 and 5 mm, a j_{app} of 40 mA cm^{-2} (2 A) was sufficient to achieve this rate. In comparison, for a d_{elec} value of 10 mm, a reduction of half of the TOC is achieved at a lower j_{app} (24 mA cm^{-2}; 1.2 A). Higher values of j_{app} are therefore not necessary at this distance.

Figure S5 highlights that flocculation is favored at large distances and large values of j_{app}. The flocculation becomes significant for j_{app} values greater than or equal to 70 mA cm^{-2} (3.5 A), which is in agreement with Faraday's law. Furthermore, the maximum sludge production reached for d_{elec} = 0.1 mm and j_{app} = 200 mA cm^{-2} (10 A) is 1.2 g. Furthermore, the flocculation per TOC removed is favored at large distances and at large j_{app} values, except at d_{elec} equal to 0.1 mm and j_{app} equal to 20 mA cm^{-2} (1 A) (**Fig. 5**). Under these latter conditions, sludge production per TOC is maximal (1891 g-sludge g-TOC^{-1}), which is related to the low TOC removal observed at this distance.

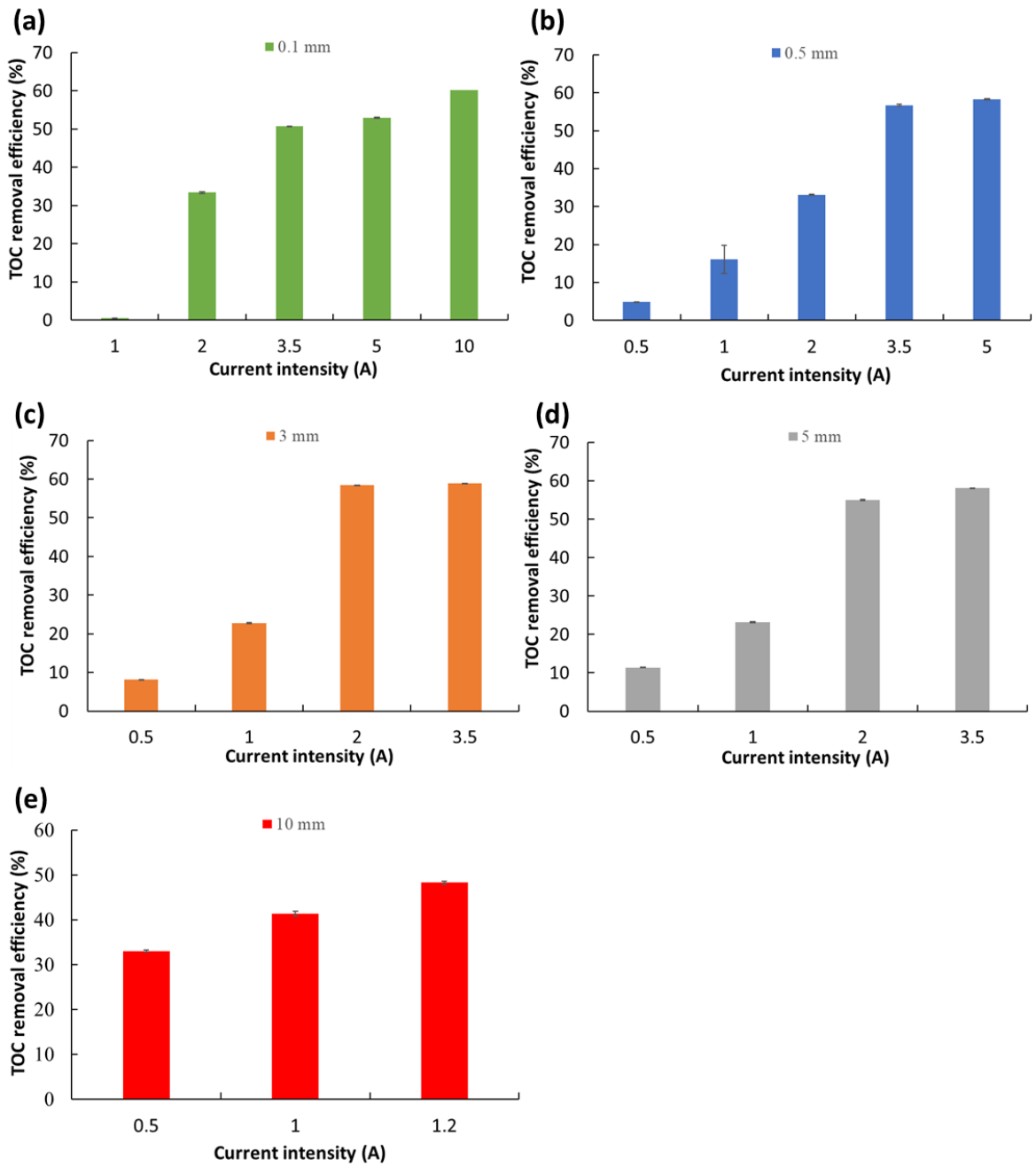

Fig. 4. Effect of I_{app} (0.5 A (10 mA cm^{-2}), 1 A (20 mA cm^{-2}), 1.2 A (24 mA cm^{-2}), 2 A (40 mA cm^{-2}), 3.5 A (70 mA cm^{-2}), 5 A (100 mA cm^{-2}), 10 A (200 mA cm^{-2})) on TOC removal yield in synthetic effluent at different d_{elec}: (a) 0.1 mm, (b) 0.5 mm, (c) 3 mm, (d) 5 mm, (e) 10 mm. Operating conditions: [paracetamol]$_0$ = 15 mg L^{-1}, [Na_2SO_4] = 568 mg L^{-1}.

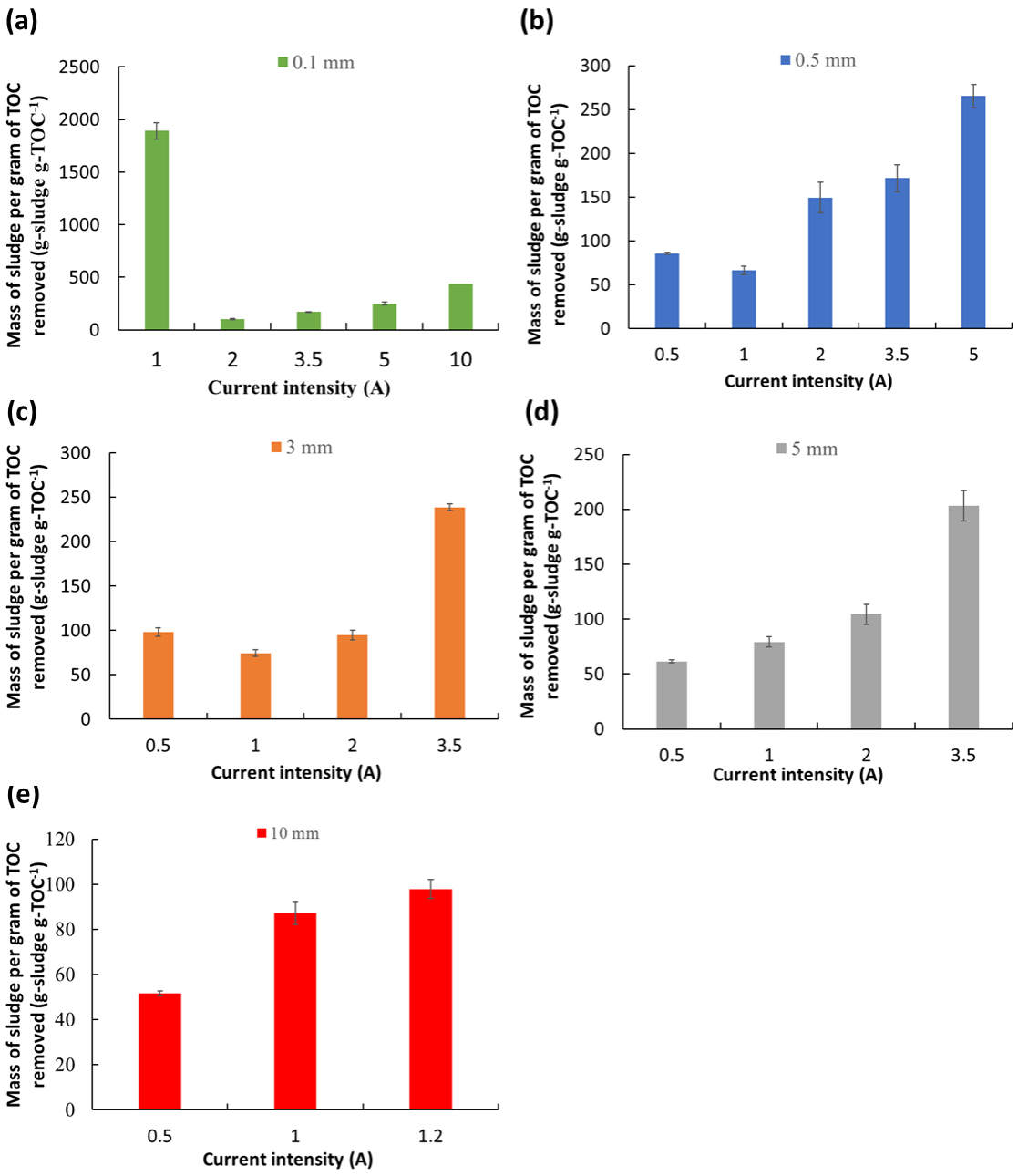

Fig. 5. Effect of I_{app} (0.5 A (10 mA cm^{-2}), 1 A (20 mA cm^{-2}), 1.2 A (24 mA cm^{-2}), 2 A (40 mA cm^{-2}), 3.5 A (70 mA cm^{-2}), 5 A (100 mA cm^{-2}), 10 A (200 mA cm^{-2})) on the mass of sludge per gram of TOC removed in synthetic effluent at different d_{elec}: (a) 0.1 mm, (b) 0.5 mm, (c) 3 mm, (d) 5 mm, (e) 10 mm. Operating conditions: $[paracetamol]_0$ = 15 mg L^{-1}, $[Na_2SO_4]$ = 568 mg L^{-1}.

Figure 6 presents the energy profile for the different experiments performed at different d_{elec} and j_{app}. This confirms that a j_{app} equal to 20 mA cm^{-2} (1 A) was the worst operating condition (158 kWh g-TOC^{-1}) for a d_{elec} of 0.1 mm. For d_{elec} between 0.5 and 10 mm, E_{sp} increased as j_{app} and d_{elec} increased. Thus, E_{sp} raised from 17.2 to 40 kWh g-TOC^{-1} at d_{elec} = 10 mm, when j_{app} increased from 10 (0.5 A) to 24 mA cm^{-2} (1.2 A). For d_{elec} = 5 mm, E_{sp} raised from 12 to 65 kWh g-TOC^{-1}, when j_{app} increased from 10 (0.5 A) to 70 mA cm^{-2} (3.5 A). For d_{elec} = 3 mm, E_{sp} increased from 16 to 44 kWh g-TOC^{-1}, when j_{app} increased from 10 (0.5 A) to 70 mA cm^{-2} (3.5 A). Finally, for d_{elec} = 0.5 mm, E_{sp} increased from 9.5 to 27 kWh g-TOC^{-1}, when j_{app} increased from 10 (0.5 A) to 100 mA cm^{-2} (5 A).

Figure S6 shows the evolution of solution pH at different d_{elec} and j_{app}. The pH of the effluent decreased regardless of the j_{app} and d_{elec} values applied, to stabilize around pH 6. These results therefore confirmed the pH trend observed in **Fig. S4**, which could perhaps be explained by the formation of by-products that acidify and buffer the medium as mentioned in Section 3.1. The evolution of the effluent conductivity during electrolysis at different d_{elec} and j_{app} is displayed in **Fig. S7**. The ionic conductivity remains relatively stable for j_{app} between 10 (0.5 A) and 40 mA cm^{-2} (2 A), with average values around 1 mS cm^{-1}. It increased for j_{app} greater than 40 mA cm^{-2} (2 A). As for the previous part, the chromatographic study is important to verify that the pollutant is well eliminated during the EC.

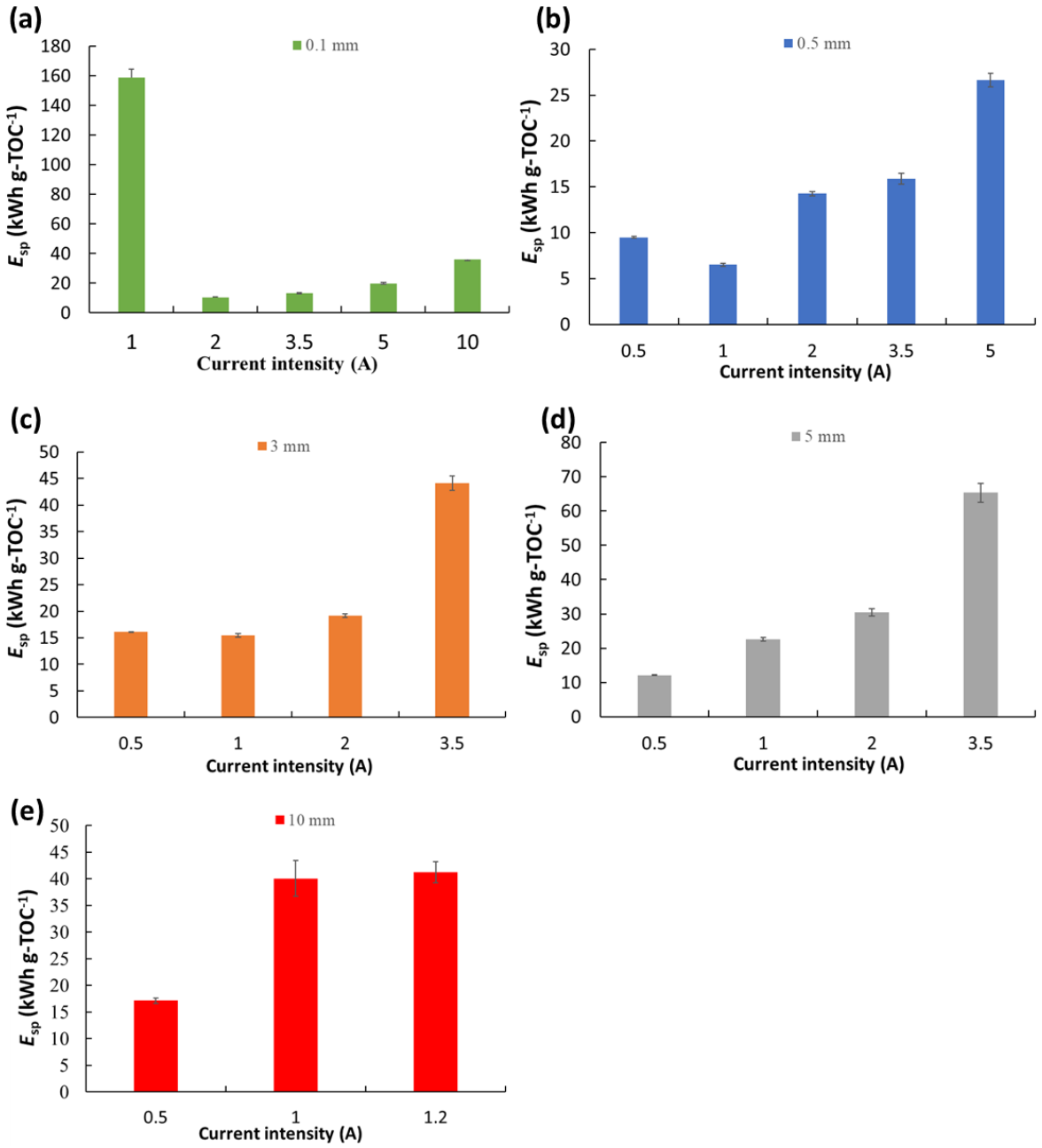

Fig. 6. Effect of I_{app} (0.5 A (10 mA cm^{-2}), 1 A (20 mA cm^{-2}), 1.2 A (24 mA cm^{-2}), 2 A (40 mA cm^{-2}), 3.5 A (70 mA cm^{-2}), 5 A (100 mA cm^{-2}), 10 A (200 mA cm^{-2})) on E_{sp} in synthetic effluent at different d_{elec}: (a) 0.1 mm, (b) 0.5 mm, (c) 3 mm, (d) 5 mm, (e) 10 mm. Operating conditions: $[paracetamol]_0$ = 15 mg L^{-1}, $[Na_2SO_4]$ = 568 mg L^{-1}.

Following these results, three optimal working conditions could be identified in EC according to the order of magnitude of the distance considered. For micro-distances, the optimal working conditions were a d_{elec} of 0.5 mm and a j_{app} of 70 mA cm^{-2} (3.5 A) (57% TOC removed, 172 g-sludge g-TOC^{-1}, 16 kWh g-TOC^{-1}). For millimetric distances, the optimal EC conditions were reached for a d_{elec} of 3 mm and a j_{app} of 40 mA cm^{-2} (2 A) (58% TOC removed, 95 g-sludge g-TOC^{-1}, 19 kWh g-TOC^{-1}). About centimetric distances, a d_{elec} of 10 mm and a j_{app} of 20 mA cm^{-2} (1 A) could be considered (41% TOC removed, 87 g-sludge g-TOC^{-1}, 40 kWh g-TOC^{-1}).

3.3. Effect of electrode materials at different interelectrode distances

The studies presented in this part are carried out with the optimal working conditions determined in section 3.2. The aim of this section is to compare the treatment performances of iron and aluminum electrodes with stainless steel at different d_{elec} including micro-distances, in order to treat real laundry effluent. The effluent was poorly conductive (~ 600 µS cm^{-1}) so a j_{app} of 20 mA cm^{-2} (1 A) could not be applied for a d_{elec} of 10 mm. A j_{app} of 10 mA cm^{-2} (0.5 A) was applied instead, which was the maximum j_{app} applicable under these conditions. This further highlights the interest of working with micro-distances for this type of poorly conductive effluent. Moreover, it was impossible to work in micro-distance with the filter press, using aluminum electrodes. This was perhaps linked to the significant production of sludge that accumulates between the cathode and the anode which ends up causing a short circuit at the reactor level.

Figure S8 shows the evolutions of the solution pH and conductivity of the laundry effluent during EC with the different electrode materials. This effluent was slightly alkaline initially (pHi = 8.9), and its pH remained substantially the same throughout the electrolysis. This observation was all the truer when the electrode material used is iron or aluminum. The results with aluminum electrodes were in agreement with the information reported in the literature (Moussa et al., 2017). This was not the case for iron and stainless steel electrodes. A decrease in pH would be usually expected with these electrodes (Moussa et

al., 2017). One or more species initially present or formed during electrolysis could capture H^+ ions, or it could be reactions that would form OH^- ions. Since a real industrial effluent was tested, the pH had more change to be buffered. This would explain this constancy in the evolution. As for the conductivity, this effluent was not very conductive and it remained substantially the same throughout the electrolysis as well.

Figure 7a shows the TOC removal rates during the electrolysis of laundry effluent obtained with iron, stainless steel and aluminum electrodes. The best TOC removal rate was achieved with aluminum electrodes. For a distance of 0.5 mm, there is no big difference between the iron and steel electrodes. However, iron is more interesting for a distance of 3 mm. These trends seemed consistent since steel also releases Fe(II)/Fe(III) ions, but as it is an alloy these performances were slightly less important than high purity iron. **Figure 7b** shows the E_{sp} during the electrolysis obtained with iron, stainless steel and aluminum electrodes. At a distance of 3 mm, iron was the material that consumed the least, then it was aluminum, and finally it was steel. Aluminum electrodes are therefore the electrodes that allow to have the highest range of elimination for an intermediate energy cost. The only problem is that they are not compatible with micro-distances, which limits their scope of application when the conductivities of the effluents are low, with this type of reactor design.

Figures S9-S12 present the kinetics of anions initially present or formed during electrolysis. It is interesting to note that no perchlorate was detected and that therefore the electro-oxidation during the EC was not powerful enough to oxidize the chlorides until perchlorate form. **Figure S9** presents the evolution of the concentrations of ClO_3^- ions formed during the electrolyses carried out with iron, aluminum and stainless steel electrodes. No concentration of ClO_3^- ions was observed with aluminum electrodes. A possible explanation could be that these ions were still formed, but they would be eliminated in the sludge produced in large quantities with this anode material. Contrastingly, with iron and stainless steel electrode materials, ClO_3^- ion concentration increased during electrolysis.

Figures S10-S12 present the evolutions of Cl^-, SO_4^{2-}, NO_3^- and PO_4^{3-} ions during electrolysis, with stainless steel, iron and aluminum electrodes, respectively. This study emphasized that the ions did not

evolve in the same way depending on the electrode material used. The different profiles that emerge are as follows:

- Aluminum electrodes were able to eliminate all the ions initially present in the effluent. This elimination was longer than with iron or steel electrodes. This was in agreement with the literature which states that the kinetic of PO_4^{3-} elimination by aluminum was longer (Yang et al., 2022). The elimination of SO_4^{2-} was long, because these ions tended to complex with aluminum, thus forming a passive layer at the anode (Trompette and Vergnes, 2009). As previously shown in the literature, NO_3^- could be adsorbed on aluminum hydroxides (Lacasa et al., 2011).

- Iron electrodes were able to eliminate all the ions initially present in the real effluent. However, the elimination of phosphate ions was not direct, and the electro-oxidation of Cl^- ions implied the production of ClO_3^- ions. The elimination of SO_4^{2-} ions was quicker with these electrodes than with aluminum electrodes. This could be explained by the fact that there was no affinity between these two species as suggested in literature (Garcia-Segura et al., 2017). There was therefore no formation of a complex passivating the iron anode that could limit the EC efficiency. Here again, NO_3^- ions were supposed to be adsorbed on iron hydroxides (Lacasa et al., 2011).

- Stainless steel electrodes can eliminate chloride and phosphate ions. However, they produced chlorate, sulfate and phosphate ions. ClO_3^- ions were notably produced by oxidation of chloride ions. NO_3^- ions were only eliminated for d_{elec} = 10 mm and j_{app} = 10 mA cm^{-2} (0.5 A).

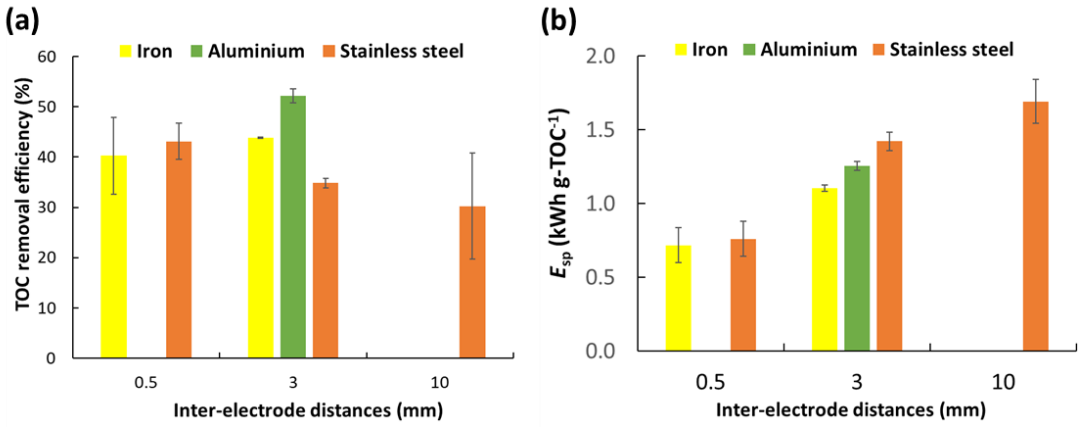

Fig. 7. Effect of anode material (iron, aluminium or stainless steel) and d_{elec} on (a) TOC removal yield and (b) E_{sp}, with real laundry effluent. Operating conditions: d_{elec} = 10 mm and I_{app} = 0.5 A, d_{elec} = 3 mm and I_{app} = 2 A, d_{elec} = 0.5 mm and I_{app} = 3.5 A.

4. Conclusions and Recommendations

The main objective of this work was to verify the viability of EC implementing micrometric d_{elec} to decrease the energy requirement and increase the removal efficiency during a separation step in WWTP, particularly with low-salinity effluents that usually involve high EC cell potential with standard centimetric d_{elec}.

Several parameters were studied and varied in order to address this goal, such as d_{elec} (0.1 - 10 mm), j_{app} (10 - 200 mA cm^{-2}) and electrode materials (iron, aluminium and 316L stainless steel). The optimal operating conditions, i.e. maximum treatment capacity, minimum sludge production and low energy consumption, were determined following the d_{elec} and j_{app} studies. Three key operating conditions with stainless steel electrodes could emerged as follows:

- d_{elec} = 10 mm and j_{app} = 20 mA cm^{-2} (41% TOC removed, 87 g-sludge g-TOC^{-1}, 40 kWh g-TOC^{-1})

- d_{elec} = 3 mm and j_{app} = 40 mA cm^{-2} (58% TOC removed, 95 g-sludge g-TOC^{-1}, 19 kWh g-TOC^{-1})

- d_{elec} = 0.5 mm and j_{app} = 70 mA cm^{-2} (57% TOC removed, 172 g-sludge g-TOC^{-1}, 16 kWh g-TOC^{-1})

These conditions were then applied in the electrode materials effect study, carried out with a real laundry effluent that has low electric conductivity (572 µS cm^{-1}). Aluminum electrodes gave the best pollutant removal rates (TOC = 52%), for an energy consumption of 1.3 kWh g-TOC^{-1}. However, their use was not possible with micro-distances, due to the limitation of the reactor design proposed. The results show that EC, which is a technology initially mainly intended to eliminate suspended solids and colloids, can nevertheless eliminate a significant quantity of organic compounds (up to 60% of TOC eliminated) and dissolved inorganic compounds. In addition, all of these studies show that micro-distances remain interesting, even in EC, for poorly conductive effluents in particular. These distances make it possible to obtain relatively high TOC elimination rates for EC (up to 60% for d_{elec} = 0.1 mm and j_{app} = 200 mA cm^{-2}), while minimizing energy consumption compared to larger distances.

Now that the impact of a wide range of d_{elec}, including micro-distances, has been newly carried out, further studies would be required to refine the optimization with Design of Experiments, particularly about the effect of electrode materials. Representative compounds that can be easily removed by coagulation-flocculation phenomena (e.g. phosphate) could be used in addition to organic pollutants such as paracetamol that has been used in this study. This will better assess the EC efficiency. Moreover, the efficiency of the system should be tested in other types of wastewater to assess the robustness of this technology. However, current reactors are not completely adapted to these distances, particularly if there is a high production of sludge. The design of a new type of reactor including micro-distances would be interesting in order to be able to exploit them in their optimal conditions without being limited by the type of electrode material to be used. The treatment of sludge is another aspect that should be monitored. Stainless steel must generate sludge containing chromium in particular, which should be avoided. Furthermore, EC is supposed to be mainly a separation step, meaning that a post-degradation step will be required to fully treat the effluents in line with the regulations before the discharge. Such treatment train will require detailed cost-efficiency analysis accompanied by a life cycle costing, life cycle assessment and life cycle sustainability assessment.

Acknowledgments

The authors would like to acknowledge Plan France Relance – ANR, a funding provided by the French government.

References

Adnan, F.H., Mousset, E., Pontvianne, S., Pons, M.N., 2021a. Mineral cathodic electro-precipitation and its kinetic modelling in thin-film microfluidic reactor during advanced electro-oxidation process. Electrochim. Acta 387, 138487. https://doi.org/10.1016/j.electacta.2021.138487

Adnan, F.H., Pons, M.-N., Mousset, E., 2022a. Thin film microfluidic reactors in electrochemical advanced oxidation processes for wastewater treatment: A review on influencing parameters, scaling issues and engineering considerations. Electrochem. Sci. Adv. 3, e2100210.

Adnan, F.H., Pons, M.-N., Mousset, E., 2021b. Mass transport evolution in microfluidic thin film electrochemical reactors: New correlations from millimetric to submillimetric interelectrode distances. Electrochem. Commun. 130, 107097. https://doi.org/10.1016/j.elecom.2021.107097

Adnan, F.H., Pontvianne, S., Pons, M.-N., Mousset, E., 2023. Role of anodically electrogenerated hydroxyl radicals in minimizing mineral cathodic electroprecipitation in the presence of hard water. Electrochem. Commun. 150, 107493. https://doi.org/10.1016/j.elecom.2023.107493

Adnan, F.H., Pontvianne, S., Pons, M.-N., Mousset, E., 2022b. Roles of H_2 evolution overpotential, materials porosity and cathode potential on mineral electro-precipitation in microfluidic reactor – New criterion to predict and assess interdependency. Electrochim. Acta 428, 140926. https://doi.org/10.1016/j.electacta.2022.140926

Adnan, F.H., Pontvianne, S., Pons, M.N., Mousset, E., 2022c. Unprecedented roles of submillimetric interelectrode distances and electrogenerated gas bubbles on mineral cathodic electro-precipitation: Modeling and interface studies. Chem. Eng. J. 431, 133413. https://doi.org/10.1016/j.cej.2021.133413

Aiyd Jasim, M., AlJaberi, F.Y., 2023. Investigation of oil content removal performance in real oily wastewater treatment by electrocoagulation technology: RSM design approach. Results Engin. 18, 101082. https://doi.org/10.1016/j.rineng.2023.101082

AlJaberi, F.Y., 2023. New design of an electrocoagulation reactor to remove pollutants from groundwater: Analysis and optimization using response surface methodology. S. Afr. J. Chem. Eng. 46, 205–216. https://doi.org/10.1016/j.sajce.2023.08.008

AlJaberi, F.Y., Alardhi, S.M., Ahmed, S.A., Salman, A.D., Juzsakova, T., Cretescu, I., Le, P.C., Chung, W.J., Chang, S.W., Nguyen, D.D., 2022. Can electrocoagulation technology be integrated with wastewater treatment systems to improve treatment efficiency? Environ. Res. 214, 113890. https://doi.org/10.1016/j.envres.2022.113890

Arbid, Y., Usman, M., Luong, N.T., Mathon, B., Cedat, B., Boily, J.F., Hanna, K., 2024. Use of iron-bearing waste materials in laundry wastewater treatment. J. Wat. Proc. Eng. 57, 104717. https://doi.org/10.1016/j.jwpe.2023.104717

Attour, A., Touati, M., Tlili, M., Ben Amor, M., Lapicque, F., Leclerc, J.P., 2014. Influence of operating parameters on phosphate removal from water by electrocoagulation using aluminum electrodes. Sep. Purif. Technol. 123, 124–129. https://doi.org/10.1016/j.seppur.2013.12.030

Brillas, E., Sirés, I., Oturan, M.A., 2009. Electro-Fenton process and related electrochemical technologies based on Fenton's reaction chemistry. Chem. Rev. 109, 6570–6631. https://doi.org/10.1021/cr900136g

Cañizares, P., Jiménez, C., Martínez, F., Rodrigo, M.A., Sáez, C., 2009. The pH as a key parameter in the choice between coagulation and electrocoagulation for the treatment of wastewaters. J. Hazard. Mater. 163, 158–164. https://doi.org/10.1016/j.jhazmat.2008.06.073

Canizares, P., Martinez, F., Rodrigo, M., Jimenez, C., Saez, C., Lobato, J., 2008. Modelling of wastewater electrocoagulation processes Part II: Application to dye-polluted wastewaters and oil-in-water emulsions. Sep. Purif. Technol. 60, 147–154. https://doi.org/10.1016/j.seppur.2007.08.005

Deng, F., Olvera-Vargas, H., Zhou, M., Qiu, S., Sirés, I., Brillas, E., 2023. Critical Review on the Mechanisms of Fe^{2+} Regeneration in the Electro-Fenton Process: Fundamentals and Boosting Strategies. Chem. Rev. 123, 4635-4662. https://doi.org/10.1021/acs.chemrev.2c00684

Diris, S., Adnan, F.H., Pons, M.N., Mousset, E., 2024. Impact of millimetric to micrometric inter-electrode distances: Is there a way to maximize the organic pollutant degradation yield and minimize the cathode scaling and chlorate formation during wastewater treatment? Electrochim. Acta 497, 144596. https://doi.org/10.1016/j.electacta.2024.144596

Ezechi, E.H., Isa, M.H., Muda, K., Kutty, S.R.M., 2020. A comparative evaluation of two electrode systems on continuous electrocoagulation of boron from produced water and mass transfer resistance. J. Wat. Proc. Eng. 34, 101133. https://doi.org/10.1016/j.jwpe.2020.101133

Feng, Q., Zhang, K., Liu, X., Guan, W., Chen, X., Song, L., Fang, F., Luo, J., Xue, Z., Jiashun, C., 2021. An improved kinetic model for dephosphorization of laundry wastewater by electrocoagulation. J. Wat. Proc. Eng. 39, 101750. https://doi.org/10.1016/j.jwpe.2020.101750

Flores, N., Brillas, E., Centellas, F., Rodríguez, R.M., Cabot, P.L., Garrido, J.A., Sirés, I., 2018. Treatment of olive oil mill wastewater by single electrocoagulation with different electrodes and sequential electrocoagulation/electrochemical Fenton-based processes. J. Hazard. Mater. 347, 58–66. https://doi.org/10.1016/j.jhazmat.2017.12.059

Garcia-Segura, S., Eiband, M.M.S.G., de Melo, J.V., Martínez-Huitle, C.A., 2017. Electrocoagulation and advanced electrocoagulation processes: A general review about the fundamentals, emerging applications and its association with other technologies. J. Electroanal. Chem. 801, 267–299. https://doi.org/10.1016/j.jelechem.2017.07.047

Hakizimana, J.N., Gourich, B., Chafi, M., Stiriba, Y., Vial, C., Drogui, P., Naja, J., 2017. Electrocoagulation process in water treatment: A review of electrocoagulation modeling approaches. Desalination 404, 1–21. https://doi.org/10.1016/j.desal.2016.10.011

Janpoor, F., Torabian, A., Khatibikamal, V., 2011. Treatment of laundry waste-water by electrocoagulation. J. Chem. Technol. Biotech. 86, 1113–1120. https://doi.org/10.1002/jctb.2625

Jing, G., Ren, S., Pooley, S., Sun, W., Kowalczuk, P.B., Gao, Z., 2021. Electrocoagulation for industrial wastewater treatment: an updated review. Environ. Sci. 7, 1177–1196. https://doi.org/10.1039/d1ew00158b

Kabdaşlı, I., Arslan-Alaton, I., Ölmez-Hancı, T., Tünay, O., 2012. Electrocoagulation applications for industrial wastewaters: a critical review. Environ. Technol. Rev. 1, 2–45. https://doi.org/10.1080/21622515.2012.715390

Khajvand, M., Drogui, P., Arab, H., Tyagi, R.D., Brien, E., 2024. Hybrid process combining ultrafiltration and electro-oxidation for COD and nonylphenol ethoxylate removal from industrial laundry wastewater. Chemosphere 363, 142931. https://doi.org/10.1016/j.chemosphere.2024.142931

Khalid, S., Wahab, A., Yasar, A., Tanveer, R., Tabinda, A.B., Zakaullah, M., 2022. Laundry wastewater treatment under detergent-free environment and reaction kinetic analysis of ozonation technique for the recycling and other applications. Desalination. Water Treat. 278, 40–48. https://doi.org/10.5004/dwt.2022.28934

Khandegar, V., Saroha, A.K., 2013. Electrocoagulation for the treatment of textile industry effluent - A review. J. Environ. Manage. 128, 949–963. https://doi.org/10.1016/j.jenvman.2013.06.043

Lacasa, E., Cañizares, P., Sáez, C., Fernández, F.J., Rodrigo, M.A., 2011. Removal of nitrates from groundwater by electrocoagulation. Chem. Eng. J. 171, 1012–1017. https://doi.org/10.1016/j.cej.2011.04.053

Lissaneddine, A., Pons, M.-N., Aziz, F., Ouazzani, N., Mandi, L., Mousset, E., 2022. A critical review on the electrosorption of organic compounds in aqueous effluent – Influencing factors and engineering considerations. Environ. Res. 204, 112128.

Li, X., Lu, S., Zhang, G., 2023. Three-dimensional structured electrode for electrocatalytic organic wastewater purification: Design, mechanism and role. J. Hazard. Mater. 445, 130524. https://doi.org/10.1016/j.jhazmat.2022.130524

Ma, P., Ma, H., Sabatino, S., Galia, A., Scialdone, O., 2018. Electrochemical treatment of real wastewater. Part 1: Effluents with low conductivity. Chem. Eng. J. 336, 133–140. https://doi.org/10.1016/j.cej.2017.11.046

Mousazadeh, M., Naghdali, Z., Al-qodah, Z., Alizadeh, S.M., Karamati, E., Malekmohammadi, S., Nidheesh, P. V, Roberts, E.P.L., 2021. A systematic diagnosis of state of the art in the use of electrocoagulation as a sustainable technology for pollutant treatment: An updated review. Sustain. Energy Technol. Assess. 47, 101353. https://doi.org/10.1016/j.seta.2021.101353

Moussa, D.T., El-Naas, M.H., Nasser, M., Al-Marri, M.J., 2017. A comprehensive review of electrocoagulation for water treatment: Potentials and challenges. J. Environ. Manage. 186, 24–41. https://doi.org/10.1016/j.jenvman.2016.10.032

Mousset, E., 2020. Unprecedented reactive electro-mixing reactor: Towards synergy between micro- and macro-reactors? Electrochem. Commun. 118, 106787. https://doi.org/10.1016/j.elecom.2020.106787

Mousset, E., Fournier, M., Su, X., 2023. Recent advances of reactive electroseparation systems for water treatment and selective resource recovery. Curr. Opin. Electrochem. 42, 101384.

Mousset, E., Frunzo, L., Esposito, G., Hullebusch, E.D. van, Oturan, N., Oturan, M.A., 2016. A complete phenol oxidation pathway obtained during electro-Fenton treatment and validated by a kinetic model study. Appl. Catal. B 180, 189–198. https://doi.org/10.1016/j.apcatb.2015.06.014

Mousset, E., Hatton, T.A., 2022. Advanced hybrid electro-separation/electro-conversion systems for wastewater treatment, reuse and recovery: compromise between symmetric and asymmetric constraints. Curr. Opin. Electrochem. 35, 101105. https://doi.org/10.1016/j.coelec.2022.101105

Nidheesh, Puthiya Veetil, Trellu, C., Vargas, H.O., Mousset, E., Ganiyu, S.O., Oturan, M.A., 2023. Electro-Fenton process in combination with other advanced oxidation processes: Challenges and opportunities. Curr. Opin. Electrochem. 37, 101171. https://doi.org/10.1016/j.coelec.2022.101171

Nidheesh, P. V., Mousset, E., Thiam, A., 2023. Recent advancements in peroxicoagulation process: An updated review. Chemosphere 339, 139627. https://doi.org/10.1016/j.chemosphere.2023.139627

Pérez, J.F., Llanos, J., Sáez, C., López, C., Cañizares, P., Rodrigo, M.A., 2018a. Development of an innovative approach for low-impact wastewater treatment: A microfluidic flow-through electrochemical reactor. Chem. Eng. J. 351, 766–772. https://doi.org/10.1016/j.cej.2018.06.150

Pérez, J.F., Llanos, J., Sáez, C., López, C., Cañizares, P., Rodrigo, M.A., 2018b. Development of an innovative approach for low-impact wastewater treatment: A microfluidic flow-through electrochemical reactor. Chem. Eng. J. 351, 766–772. https://doi.org/10.1016/j.cej.2018.06.150

Pérez, J.F., Llanos, J., Sáez, C., López, C., Cañizares, P., Rodrigo, M.A., 2017. A microfluidic flow-through electrochemical reactor for wastewater treatment: A proof-of-concept. Electrochem. Commun. 82, 85–88. https://doi.org/10.1016/j.elecom.2017.07.026

Radjenovic, J., Sedlak, D.L., 2015. Challenges and opportunities for electrochemical processes as next-generation technologies for the treatment of contaminated water. Environ. Sci. Technol. 49, 11292–11302. https://doi.org/10.1021/acs.est.5b02414

Ren, G., Zhou, M., Su, P., Liang, L., Yang, W., Mousset, E., 2018. Highly energy-efficient removal of acrylonitrile by peroxi-coagulation with modified graphite felt cathode: Influence factors, possible mechanism. Chem. Eng. J. 343, 467–476. https://doi.org/10.1016/j.cej.2018.02.115

Richardson, S.D., Ternes, T.A., 2014. Water analysis: emerging contaminants and current issues. Anal. Chem. 86, 2813–48. https://doi.org/10.1021/ac500508t

Rizzo, L., Gernjak, W., Krzeminski, P., Malato, S., McArdell, C.S., Perez, J.A.S., Schaar, H., Fatta-Kassinos, D., 2020. Best available technologies and treatment trains to address current challenges in urban wastewater reuse for irrigation of crops in EU countries. Sci. Tot. Environ. 710, 136312. https://doi.org/10.1016/j.scitotenv.2019.136312

Rodier, J., Legube, B., Merlet, N., 2009. Analyse de l'eau (Water analysis), ninth. ed. Dunod, Paris. (in French).

Rodríguez, M., Muñoz-Morales, M., Perez, J.F., Saez, C., Cañizares, P., Barrera-Díaz, C.E., Rodrigo, M.A., 2018. Toward the Development of Efficient Electro-Fenton Reactors for Soil Washing Wastes through Microfluidic Cells. Ind. Eng. Chem. Res. 57, 10709–10717. https://doi.org/10.1021/acs.iecr.8b02215

Sabatino, S., Galia, A., Scialdone, O., 2016. Electrochemical abatement of organic pollutants in continuous-reaction systems through the assembly of microfluidic cells in series. ChemElectroChem 3, 83–90. https://doi.org/10.1002/celc.201500409

Sánchez Calvo, L., Leclerc, J.P., Tanguy, G., Cames, M.C., Paternotte, G., Valentin, G., Rostan, A., Lapicque, F., 2003. An electrocoagulation unit for the purification of soluble oil wastes of high COD. Environ. Progr. 22, 57–65. https://doi.org/10.1002/ep.670220117

Scialdone, O., Corrado, E., Galia, A., Sirés, I., 2014. Electrochemical processes in macro and microfluidic cells for the abatement of chloroacetic acid from water. Electrochim. Acta 132, 15–24. https://doi.org/10.1016/j.electacta.2014.03.127

Scialdone, O., Galia, A., Sabatino, S., 2013. Electro-generation of H_2O_2 and abatement of organic pollutant in water by an electro-Fenton process in a microfluidic reactor. Electrochem. Commun. 26, 45–47. https://doi.org/10.1016/j.elecom.2012.10.006

Scialdone, O., Guarisco, C., Galia, A., 2011. Oxidation of organics in water in microfluidic electrochemical reactors: Theoretical model and experiments. Electrochim. Acta 58, 463–473. https://doi.org/10.1016/j.electacta.2011.09.073

Scialdone, O., Guarisco, C., Galia, A., Filardo, G., Silvestri, G., Amatore, C., Sella, C., Thouin, L., 2010. Anodic abatement of organic pollutants in water in micro reactors. J. Electroanal. Chem. 638, 293–296. https://doi.org/10.1016/j.jelechem.2009.10.031

Song, D., Kadier, A., Peralta-Hernández, J.M., Xie, H., Hao, B., Ma, P.C., 2022. Separation of oil-water emulsions by a novel packed bed electrocoagulation (EC) process using anode from recycled aluminum beverage cans. J. Clean Prod. 379, 134693. https://doi.org/10.1016/j.jclepro.2022.134693

Trompette, J.L., Vergnes, H., 2009. On the crucial influence of some supporting electrolytes during electrocoagulation in the presence of aluminum electrodes. J. Hazard. Mater. 163, 1282–1288. https://doi.org/10.1016/j.jhazmat.2008.07.148

Vargas, A.R., Haynes, M.E.M., Guillen, C.S., Aljaberi, F.Y., 2023. Removal of nickel from Ni(II)-NH_3-SO_2-CO_2-H_2O system by electrocoagulation, sedimentation and filtration processes. J. Electrochem. Sci. Eng. 13, 373–391. https://doi.org/10.5599/jese.1376

Wang, Z., Shen, Q., Xue, J., Guan, R., Li, Q., Liu, X., Jia, H., Wu, Y., 2020. 3D hierarchically porous NiO/NF electrode for the removal of chromium(VI) from wastewater by electrocoagulation. Chem. Eng. J. 402, 126151. https://doi.org/10.1016/j.cej.2020.126151

Yang, Y., Li, Y., Mao, R., Shi, Y., Lin, S., Qiao, M., Zhao, X., 2022. Removal of phosphate in secondary effluent from municipal wastewater treatment plant by iron and aluminum electrocoagulation: Efficiency and mechanism. Sep. Purif. Technol. 286, 120439. https://doi.org/10.1016/j.seppur.2021.120439